Classical Studies of H Atom Trapping on a Graphite Surface†

Jay Kerwin, Xianwei Sha, and Bret Jackson*

Department of Chemistry, University of Massachusetts, Amherst, Massachusetts 01003

Received: December 7, 2005; In Final Form: February 9, 2006

The trapping and sticking of H and D atoms on the graphite (0001) surface is examined over the energy range 0.1−0.9 eV. Total electronic energy calculations based on density functional theory are used to develop a potential energy surface that allows for the full three-dimensional motion of the incident atom and the reconstruction of the bonding carbon atom, which must pucker out of the surface to form a stable bond. Classical methods are used to compute trapping cross sections as a function of incident energy. The C−H bond, once formed, rapidly dissociates without a mechanism to dissipate its excess energy. However, a number of long-lived trapping resonances exist, and for impact parameters below 1 Å or so, several percent of the incident H atoms can remain trapped for 1 ps or more. This long-time trapping probability increases significantly when additional lattice degrees of freedom are added to carry energy away from the C−H stretch. Trapping can also increase with an increasing collision impact parameter, as H vibrations parallel to the surface become excited, leaving less energy in the C−H stretch. The trapping cross section at 1 ps reaches a maximum of 0.2 Å^2 for an H atom energy of 0.3 eV. Assumimg that any atoms remaining trapped after 1 ps fully relax and stick, we estimate a lower bound for the sticking probability of H and D to be 0.024 and 0.050, respectively, about an order of magnitude below the experimental values.

I. Introduction

Much effort has been directed toward understanding the interactions of hydrogen atoms with graphite surfaces. Interest in this area has been sparked by such topics as the erosion of the graphite-lined walls in fusion reactors,[1] the storage of hydrogen in carbon-based materials,[2] and the interstellar formation of H_2.[3] The mechanistic details of H_2 formation in interstellar space remain unclear, though it is generally believed that H recombination happens on the surface of dust grains,[3] which are known to contain graphitic components.[4] The mechanism of this process is thought to be primarily Eley−Rideal, where a gas phase H atom reacts more-or-less directly with an adsorbed H atom, but Langmuir−Hinshelwood pathways may contribute as well.

Several recent electronic structure studies of the chemisorption of H atoms on graphite have demonstrated that H can form a chemical bond to a carbon atom on the basal plane of graphite, with a binding energy of about 0.67 eV, but that a significant amount of surface reconstruction is necessary.[5−9] The bonding carbon atom must pucker out of the surface plane by 0.36 Å, leading to a barrier to sticking of about 0.25 eV. Following this work, numerous theoretical studies have appeared of H atom adsorption and diffusion.[10−13] The reactions of H atoms with these adsorbed H atoms to form H_2 via Eley−Rideal[14−22] and Langmuir−Hinshelwood[23] mechanisms have also been examined theoretically. Quantum mechanical studies of the Eley−Rideal reaction have suggested that the cross sections are large—on the order of 10 Å^2—in agreement with earlier model predictions.[17] Zecho et al. were the first to demonstrate experimentally that H could indeed chemisorb on the basal plane of graphite, and they found evidence for puckering of the surface.[24] The vibrational frequencies of these adsorbed atoms[24] and the Eley−Rideal abstraction cross sections[25] were both measured and found to be in excellent agreement with theory.[20,24,25] In addition, the measured barrier to sticking of 0.2 ± 0.1 eV[26] was consistent with earlier predictions.[5−8] Other laboratory studies are currently examining these adsorption and abstraction processes.[27]

Zecho et al. also measured sticking probabilities of H and D on graphite of 0.4 ± 0.2, at a surface temperature of 150 K.[24] These are surprisingly large, given that it is not obvious that the bonding carbon atom should have the time to distort by several tenths of an angstrom during the brief H−surface collision. In an earlier study, the dynamics of this event were examined using a quantum model in which both the H atom and the bonding carbon were restricted to motion normal to the surface in a collinear configuration.[28] This simple model suggested that sticking may proceed via a trapping resonance, in which a vibrationally excited C−H complex was formed. The lifetimes of these resonances were computed, and some were found to be stable for several picoseconds. An additional lattice mode was added to carry energy away from the excited C−H complex, and the addition of this mode significantly increased the amount of adsorbed H remaining after 1 ps of propagation time. While this simple collinear study has helped to elucidate the mechanism for H sticking, to compare directly with experiments, one needs to compute sticking cross sections.

In this paper, we examine this problem in greater detail. In section II, we present the results of total energy calculations based on density functional theory (DFT), where the H−graphite interaction is examined as a function of both the H atom location and the displacement of the bonding carbon. A potential energy surface (PES) is then constructed, which allows for the fully three-dimensional motion of the H atom, as well as additional lattice degrees of freedom. In section III, classical trajectory methods are used to examine the trapping process. The classical

† Part of the special issue "Robert J. Silbey Festschrift".

* To whom correspondence should be addressed. Electronic mail: jackson@chem.umass.edu.

10.1021/jp057136+ CCC: $33.50
Published on Web 03/17/2006

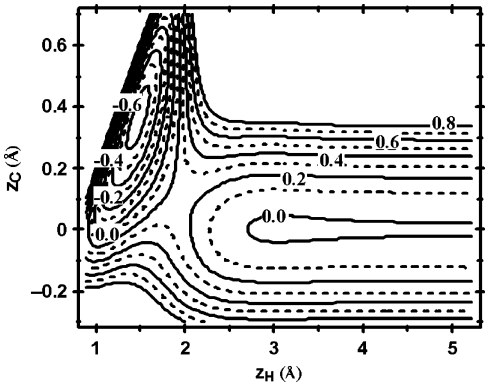

Figure 1. Potential energy contours for the collinear configuration, as a function of z_H, the distance of the H atom above the surface plane, and z_C, the height of the carbon above the surface. The contour spacing is 0.1 eV, and the contour labels are in eV.

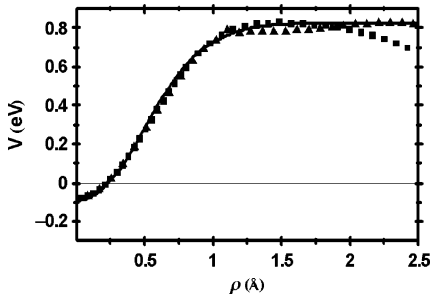

Figure 2. Potential energy as a function of ρ, for $z_H = 1.656$ Å and $z_C = 0.2$ Å. The solid line is from the model, and the symbols are from the DFT calculations. The triangles and squares correspond to the H moving toward the neighboring carbon and toward the hollow site, respectively.

results are compared with the quantum for the lower dimensional collinear model, and cross sections for trapping are computed for the higher dimensional PES. We conclude with a summary and a comparison with the experiments in section IV.

II. Model

Our model consists of an H atom incident on a graphite (0001) surface. As a first approximation, only the H atom and the carbon to which the H atom bonds will be allowed to move. The H atom coordinates are z_H, its distance above the plane of the surface, and x_H and y_H, which describe its location over the surface plane relative to the bonding carbon. The bonding carbon is only allowed to move normal to the surface, and z_C is the displacement of this carbon atom out of the surface plane. Total energies, V_T, were computed for numerous values of z_H, x_H, y_H, and z_C using the well-established DFT code VASP (Vienna ab initio simulation package) developed at the Institut für Materialphysik of the Universität Wien.[29−31] This package uses a plane wave basis set, and nonlocal exchange-correlation effects are introduced via a generalized gradient approximation, using the Perdew−Wang functional PW91.[32] Spin-polarized calculations have been performed. A four-layer slab supercell is used to model the graphite, with eight carbon atoms per layer. We direct the reader to ref 7 for more details.

We find that our total PES, V_T, can be constructed from two limiting forms, V_0 and V_i. $V_0(z_H, z_C)$ is the energy for the collinear configuration, where the H atom is restricted to be directly over the bonding carbon ($x_H = 0$ and $y_H = 0$), and V_i is the energy when the H atom is very far away from the bonding carbon (x_H and y_H go to infinity). To determine $V_0(z_H, z_C)$, total energy DFT calculations were performed for 21 different values of z_C, at each of 35 different values of z_H. An analytical form for $V_0(z_H, z_C)$ described in Appendix A was then fit to these 735 energies.

In Figure 1, we plot our analytical collinear PES, V_0. Note that for the flat surface ($z_C = 0$) there is a quasi-bound state near $z_H = 1.2$ Å but no stable chemisorption. As the bonding carbon moves out of the surface plane ($z_C > 0$) and toward the incoming H atom, a stable chemical bond begins to form. For our analytical PES, the maximum binding energy of 0.66 eV occurs for $z_C = 0.37$ Å and there is a barrier to chemisorption of about 0.24 eV. These values, and the overall PES, are in good agreement with the collinear PES used in our earlier study (Figure 1 of ref 28), which was spline fit directly to our DFT energies. Our collinear PES is also consistent with the work of Sidis and co-workers,[6] who performed similar DFT calculations using a cluster model with an atomic orbital basis set. The model vibrational frequencies for chemisorbed H and D are in good agreement with those measured by the Küppers group,[24] and our barrier to chemisorption agrees well with the value measured by that group, 0.2 ± 0.1 eV.[26]

We found, for a fixed z_C and z_H, that the total energy V_T depended primarily upon $\rho = \sqrt{x_H^2 + y_H^2}$, the radial distance of the H atom from the bonding carbon along the plane of the surface, and only very weakly on the particular direction it moved along the surface. This can be seen clearly in Figure 2, where we plot total DFT energies as a function of ρ, for $z_H = 1.656$ Å and $z_C = 0.2$ Å. Plotted are results for the H moving in two different directions: toward a neighboring carbon along a C−C bond and in a direction between two neighboring carbons, toward the hollow site. We see that for ρ less than 1 Å or so, the energy is independent of the direction of the moving H atom along the plane of the surface. At larger values of ρ, there is a weak corrugation effect, but H atoms in this region of the PES are too far away to interact with the bonding carbon. Remember that only a single carbon is reactive in our model. This is a good approximation when the H atom does not significantly interact (chemically) with more than one carbon at a time, which is certainly the case here. In this case, the trapping probability is the single-carbon trapping cross section, divided by the surface area per C atom. We, thus, adopt a cylindrical form for V_T. For small values of ρ, the PES is harmonic to a good approximation, and the force constant k_ρ was computed via DFT at 21 relevant locations in the (z_H, z_C) plane. An analytical form for the function $k_\rho(z_H, z_C)$ was then fit to these values of k_ρ, as described in Appendix A.

Our total PES is well described by the following form:

$$V_T(z_H, z_C, \rho) = \left[V_0(z_H, z_C) + \frac{1}{2}k_\rho(z_H, z_C)\rho^2\right][1 - s(\rho)] + [(V_i(z_H, z_C) - V_0(z_H, z_C))f(\rho) + V_i(z_H, z_C)]s(\rho) \quad (1)$$

The switching function, $s(\rho)$, where

$$s(\rho) = [1 + \exp(-b_s(\rho - \rho_s))]^{-1} \quad (2)$$

connects the PES at small values of ρ to that at large values. The function, $f(\rho)$, where

$$f(\rho) = \exp[-2a_f\rho] - 2\exp[-a_f\rho] \times \exp[-b_f\rho/(1 + \exp\{-c_f(\rho - \rho_f)\})] \quad (3)$$

describes the ρ behavior at large ρ. Note that for a collinear configuration of the H atom and the bonding carbon ($\rho = 0$), we have that $f(0) = -1$, and $V_T = V_0$. For ρ going to infinity,

the asymptotic form of the PES is

$$V_i(z_H,z_C) = D_i[\exp[-2\alpha_i(z_H - a_i)] - 2\exp[-\alpha_i(z_H - a_i)]] + {}^1/_2 k_C z_C{}^2 \quad (4)$$

where, again, we ignore the weak surface corrugation. The Morse parameters describing the laterally averaged H-graphite physisorption interaction, the force constant for the carbon vibration, k_C, and the parameters defining $s(\rho)$ and $f(\rho)$ were fit to the DFT total energies and are listed in Appendix A. The resulting total PES, V_T, is plotted in Figure 2 as the solid line, and we see that the agreement with the DFT points is good in the region where the trapping takes place, and reasonable otherwise. Because the H atom is free to move in three dimensions, we will refer to our studies using V_T as the "3D" model, to distinguish from our "collinear" studies based on V_0.

It is important to distinguish between trapping and sticking. Our model Hamiltonian contains no dissipative terms, and the total energy is conserved. Thus, we can only describe trapping, since for a positive H atom incident energy the total energy of the graphite−H complex is positive, and the H atom will eventually desorb, even though it may remain bound for 1 ps or more. True sticking requires that the excess energy in the C−H stretch be dissipated into the excitations of the substrate. We will estimate sticking from our time dependent trapping simulations, assuming lattice relaxation times on the order of a ps. Clearly, the amount of sticking depends on the rate at which the excited C−H bond dissociates vs the rate at which this excited vibration dissipates its energy into the lattice modes. To help carry energy away from and stabilize the trapped H and to improve our estimate of the fraction of H atoms that should remain trapped at long times, we include an extra lattice degree of freedom, Q. Q corresponds to the displacement of the lattice atoms surrounding the bonding carbon from their equilibrium positions, normal to the surface, where $Q > 0$ is away from the graphite substrate. Since the bonding carbon vibrates relative to this surrounding lattice, the full Hamiltonian for the "3D+Q" model can be written:

$$H = \frac{|p_H|^2}{2m_H} + \frac{p_C{}^2}{2m_C} + \frac{p_Q{}^2}{2m_Q} + V_T(z_H - Q, z_C - Q, p) + \frac{1}{2}m_Q\omega_Q{}^2Q^2 \quad (5)$$

were m_H, m_C, and m_Q are the masses of the H and C atoms and the effective mass of the additional lattice vibration, respectively. The moments p_H, p_C, and p_Q describe the H, C, and Q motion, with dimensionalities of 3, 1, and 1, respectively. The "collinear+Q" model is defined in a similar fashion. The optical phonon mode with its displacement normal to the surface should couple most strongly,[33] and we thus take $\hbar\omega_Q = 0.11$ eV. We also use $m_Q = 12$ amu. Other phonons can be important, of course, and in our earlier study, we examined the effects of changing this frequency over a relatively wide range and varying m_Q between 12 and 36 amu. These changes were found to not significantly modify the trapping dynamics,[28] which is not surprising considering the large amounts of energy involved.

We consider H and D atoms, at normal incidence, with energies in the range 0.1−0.9 eV. As we are primarily interested in the terrestrial experiments of Küppers and co-workers,[24,25] we will not explore the extremely low energies relevant to H chemisorpion in interstellar space. We use a standard velocity-Verlet algorithm to integrate the classical equations of motion. Typically, 2000 trajectories are integrated for each of 250 values for the impact parameter b, ranging from 0 to 2.5 Å. At $t = 0$, when the H atom is far above the surface, V_T describes a pair of coupled oscillators along the Q and z_C coordinates. As in our earlier study, we diagonalize to find the proper normal coordinates and normal modes. In that work, we showed that the normal-mode frequencies were large relative to typical experimental values of kT and that the thermally averaged 300 K results did not vary much from the $T = 0$ K results.[28] In this work, we thus take these normal vibrations to be in the ground state and use standard quasi-classical methods to include the vibrational zero point energies. For our choice of $\hbar\omega_Q$ and m_Q, the total lattice (z_C and Q) vibrational zero point energy is 117 meV.

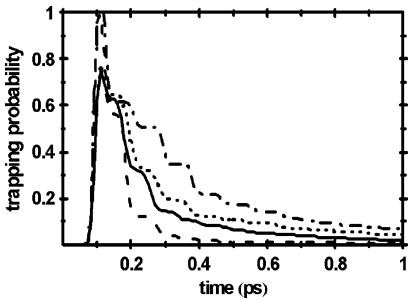

Figure 3. Trapping probability as a function of time, for H with an incident energy E_i of 0.3 eV. The quantum results for the collinear and collinear+Q models are plotted as the solid and dotted lines, respectively. The classical results for the collinear and collinear+Q models are plotted as the dashed and dotted−dashed lines, respectively.

III. Results and Discussion

We begin by comparing our classical results with the quantum results, for both the collinear and collinear+Q cases. Our new analytical PES is used, so the quantum results presented here are slightly different from those presented in the earlier study.[28] Given that there is a barrier and that trapping resonances are involved, quantum effects can be important, especially for these lower-dimensional cases. In Figure 3, we plot the trapping probability as a function of time, for H with an incident energy E_i of 0.3 eV. For the classical calculations, we define the trapping probability as the fraction of all trajectories at a propagation time t with $z_H \leq 2.5$ Å, which corresponds approximately to H being in the chemisorption region. For the quantum calculations, the trapping probability is set equal to the square of the wave function integrated over the region of configuration space defined by $z_H \leq 2.5$ Å. The quantum calculation uses a Gaussian wave packet to represent the incident atom, and for this comparison, the initial momenta of the incident H atom trajectories in the classical calculation are selected from an equivalent Gaussian distribution.

All four curves in Figure 3 exhibit the same qualitative behavior. Initially, a significant fraction of the H atoms cross the barrier, but many reflect back before the carbon has time to fully reconstruct. The forces on the bonding carbon atom are large, however, and the lattice can pucker fully in about 40 fs. At this energy, roughly 60% of the incident H atoms remain trapped for at least one vibration of the C−H stretch. As the excited C−H or Q−C−H complex oscillates, it slowly dissociates, with the H atoms eventually scattering back into the gas phase. The "stepped" features in Figure 3 correspond roughly to the vibration of the carbon atom (collinear case) or the normal mode composed primarily of the carbon vibration (collinear+Q case); i.e., the H atom is most likely to leave when the oscillating carbon is near the plane of the surface (see Figure 1). Because

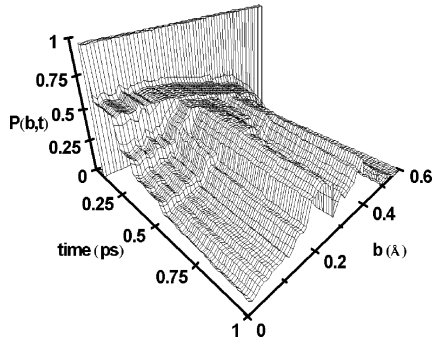

Figure 4. Trapping probability $P(b, t)$, for H with an incident energy of 0.3 eV, for the 3D+Q case, as a function of both time and the impact parameter b.

our finite model system can only describe trapping, and not sticking, the energy remains positive and the C−H bond will eventually break, with the H desorbing. The trapped part of our wave function consists of a linear combination of trapping resonances, the quasi-bound eigenstates of H, and in a previous study, the energies and lifetimes for these states were calculated for the collinear case.[28] Many are short-lived, and thus in Figure 3, we see that most of the trapped H atoms desorb within a few hundred femtoseconds. However, some of these resonances have lifetimes of several picoseconds, and thus, the trapping probability decays much more slowly at longer times. Inclusion of the additional lattice coordinate, Q, increases the trapping probability at long times. This extra degree of freedom takes energy away from the excited C−H stretch, helping to stabilize it. Put another way, this higher dimensional system has a higher density of trapping resonances, with generally larger lifetimes. The trapping probability at long times, say 1 ps, should roughly correspond to the sticking probability, since any H atoms remaining on the surface after this time should have been able to dissipate their excess energy into the phonons or electron hole pair excitations of the substrate.

While the quantum and classical results exhibit the same behavior, the agreement is certainly not perfect. The results in Figure 3 are typical in that the quantum−classical comparison is generally not better or worse at the other energies examined. In addition, the quantum trapping probabilities are not consistently either larger or smaller than the classical ones. Again, given the barrier and the important role played by resonances, this is not surprising. However, the classical results exhibit the correct physical behavior and are in reasonable agreement with the quantum ones. While it is important to continue to develop higher dimensional quantum treatments of this problem, the classical approach allows us to add two more degrees of freedom to the H atom motion and additional lattice modes. We also expect that the classical−quantum comparison will improve as we move to these higher dimensional systems.

In Figure 4, we plot $P(b, t)$, the trapping probability for the 3D+Q case as a function of both time and the impact parameter b, the initial value of ρ. The incident energy E_i is 0.3 eV. For the higher dimensional results in this, and all remaining figures, we use a single incident H atom momentum corresponding to E_i, since there are no quantum wave packet results to compare with. We can note several interesting things. First, there are significant contributions from noncollinear trajectories, for b as large as 0.5 Å or so. We see in Figure 2 that the PES is attractive with respect to ρ, for $\rho < 1$ Å, and that noncollinear trajectories can steer into the reacting carbon. These trajectories make significant contributions to the trapping cross section, σ, where

$$\sigma(t) = \int_0^{2\pi}\int_0^{\infty} P(b, t) b \, db \, d\phi = 2\pi \int_0^{\infty} P(b, t) b \, db \quad (6)$$

due to the larger weighting at larger b. Because of this steering, some of the incident kinetic energy is converted into motion of the H atom parallel to the surface. This results in vibrational excitation of the adsorbed H atom parallel to the surface plane, with correspondingly less energy being available for the C−H stretch. We thus see a significant increase in $P(b, t)$ at longer times for $b > 0$, with the highest trapping probabilities at $t =$ 1 ps arising from trajectories with values of b between 0.2 and 0.4 Å.

In Figure 5, we examine this steering effect in greater detail, plotting the trapping probability at 1 ps as a function of the impact parameter, over the full range of energies. At the lower energies, the major contributions are from trajectories with impact parameters between about 0.2 and 0.5 Å, as seen in Figure 4. However, as the incident energy increases, the cross section becomes dominated by trajectories with increasingly larger impact parameters. At $E_i = 0.9$ eV, for example, most of the H atoms still trapped at 1 ps correspond to trajectories with b approximately 0.8 Å. The observed behavior arises from the fact that, at larger impact energies, more vibrational excitation of the trapped H parallel to the surface is required to keep the C−H bond from breaking. Only the larger impact parameter collisions have sufficient parallel vibrational excitation of the H to remain trapped at 1 ps. Of course, steering is less effective at these larger energies, and the trapping probability becomes very small by $E_i = 0.9$ eV.

In Figure 6, we plot the trapping cross section, σ, as a function of time, for incident H atom energies of 0.3, 0.4, and 0.5 eV. Not surprisingly, we typically observe increased barrier crossing and more trapping at shorter times as we increase E_i. However, for higher total energies, there is more energy in the C−H stretch and the complex dissociates more rapidly, as illustrated in Figure 5. Put another way, at larger values of E_i we populate more of the higher energy shorter lifetime trapping resonances and less of the longer-lived lower energy resonances near the barrier. The overall effect is that long-time trapping, and thus sticking, decreases as the incident energy is raised above about 0.3−0.4 eV.

In Figure 7, we plot the trapping cross section at $t = 1.0$ ps as a function of the incident energy E_i, for both the 3D and 3D+Q cases. As for the collinear studies, there is a significant increase in long-time trapping when the lattice surrounding the bonding carbon is allowed to vibrate and carry energy away from the C−H stretch. The trapping cross section rises rapidly with energy, once E_i exceeds the barrier height. As the energy increases, however, increased excitation of the C−H stretch leads to shorter lifetimes for the trapped state. The result is that long-time trapping is limited to a relatively narrow range of energy. As in the collinear studies, there is interesting structure in the plots of σ vs E_i, and the peaks may correspond to the locations of the longest-lived trapping resonances. We in fact see more structure here than in the quantum calculations of ref 28, though a wave packet with an energy uncertainty of 35 meV at $E_i = 0.3$ eV was used in those studies, while the classical results shown here have no initial uncertainty in the energy. If we repeat these classical calculations using the same energy uncertainty, the plots in Figures 7 and 8 become smooth.

If we equate the trapping cross section at 1 ps to the sticking cross section, then given the surface area per carbon atom on a graphite (0001) surface, the value of σ at $t = 1$ ps and $E_i = 0.3$ eV, 0.2 Å^2, corresponds to a sticking coefficient (probability) of 0.08. To compare more directly with the experiment, where

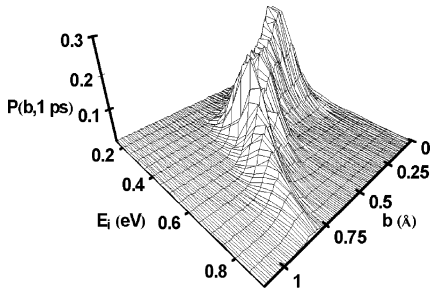

Figure 5. Trapping probability $P(b, t)$, for H at time $t = 1$ ps, as a function of both the incident energy and the impact parameter b.

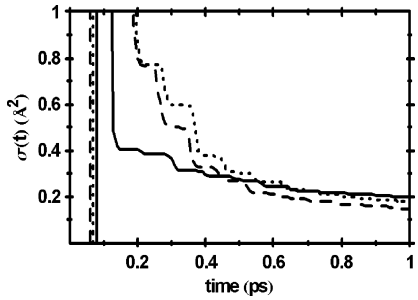

Figure 6. Trapping cross section, σ, as a function of time, for an incident H atom at three energies: 0.3 eV (solid line), 0.4 eV (dashed line), and 0.5 eV (dotted line).

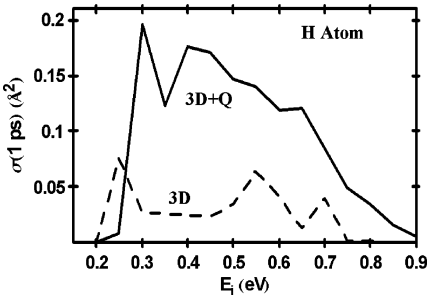

Figure 7. Trapping cross section for H at 1.0 ps, as a function of the incident energy, for both the 3D and 3D+Q cases, as indicated.

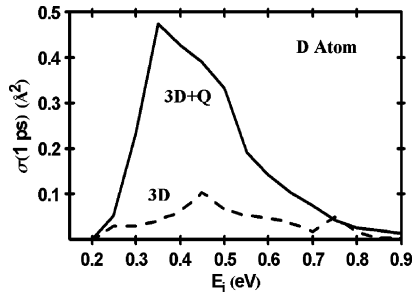

Figure 8. Trapping cross section for D at 1.0 ps, as a function of the incident energy, for both the 3D and 3D+Q cases, as indicated.

H atoms originate from a heated tungsten filament, we weight our σ ($t = 1$ ps) results using a normalized Boltzmann distribution for a 2000 K source. For the 3D+Q case, the thermally averaged sticking cross section is then 0.06 Å^2, corresponding to a zero coverage sticking coefficient for H of $s_0 = 0.024$. While this result is not in good agreement with the experimental value of 0.4 ± 0.2, our estimate of 0.024 is certainly a lower bound. First, Figure 7 clearly shows that the addition of a single extra lattice mode Q increases the trapping cross section significantly. Inclusion of additional modes will no doubt increase this value further. Second, the choice of 1 ps to define sticking is clearly arbitrary. Dissipation of energy away from the $Q-$C$-$H complex and into the substrate excitations begins immediately upon trapping, and the relaxation may be complete well before this time, further increasing our estimate of s_0. We also note that our 2000 K Boltzmann distribution peaks around 0.17 eV, and given our barrier height of 0.24 eV, roughly half of the incident atoms cannot even cross the barrier to trap or stick. The experimental barrier height, on the other hand, is estimated at 0.2 ± 0.1 eV,[26] and while our barrier is certainly within the error bars of the experiment, lowering its value to 0.20 eV or less would greatly increase our thermally averaged sticking coefficient. It is well-known, in fact, that DFT with the PW-91 functional tends to overestimate barriers.

We consider the trapping of D atoms in Figure 8. For the $Q = 0$ case, the trapping is fairly similar to that for H, except that the locations of the resonances shift. As for H, the inclusion of the additional lattice coordinate Q significantly increases the trapping at long times. For the 3D+Q case, the overall behavior is qualitatively similar to that for H, but the trapping cross sections are roughly twice as large at energies just above the barrier. This is not unexpected, since the relevant mass ratios are twice as large and the incident D more effectively transfers energy to both the bonding carbon and the vibration described by Q. In addition, the larger mass of D leads to a larger density of states for the trapping resonances and longer lifetimes. However, the trapping is not significantly larger for D than for H. Making the same arguments as in the preceding paragraph, we estimate that the thermally averaged D atom trapping cross section is 0.13 Å^2, corresponding to a zero coverage sticking coefficient of $s_0 = 0.050$ for the 3D+Q case.

IV. Summary

In conclusion, we have used classical trajectory methods to examine the trapping and sticking of H and D atoms on the graphite (0001) surface. Total electronic energy calculations based on density functional theory were used to develop a potential energy surface allowing for the full three-dimensional motion of the incident atom and the reconstruction of the bonding carbon atom. For hydrogen to chemisorb, the bonding carbon must pucker out of the surface plane by 0.36 Å. For incident energies above the 0.24 eV barrier, a significant fraction of the incident atoms can trap, forming a highly excited C$-$H bond. This bond rapidly dissociates over a few hundred femtoseconds, with the H atom desorbing. However, a number of long-lived trapping resonances exist, and for impact parameters below 1 Å or so, several percent of the incident H atoms can remain trapped for several picoseconds or more. This long-time trapping probability increases significantly when additional lattice degrees of freedom, which carry energy away from the excited C$-$H stretch, are added to the model.

From our 3D+Q results at 1 ps, we can estimate a lower bound to the sticking probability. The sticking of H rises rapidly with the incident energy E_i, for E_i above the barrier, to a maximum of 8% at $E_i = 0.3$ eV. Sticking then drops with E_i as the C$-$H stretch becomes more excited, more unstable, and harder to relax. The sticking arises from three sources: First, the forces on the bonding carbon are large, and the lattice can rapidly reconstruct in the presence of the H, within about 50 fs. Second, energy is very rapidly carried away from the C$-$H stretch into other modes of the lattice. Third, trajectories at nonzero impact parameters can react due to a steering mechanism. These contributions to the reactivity at larger impact parameters significantly increase the cross section. In addition, this steering leads to vibrational excitation of the H atom parallel to the surface, leaving less energy in the C$-$H stretch and stabilizing the system.

The experiments report that there is no sticking at low incident energies (below about 0.15 eV), and this is consistent with our calculations.[24,34] The experiments, for a surface temperature of 150 K, report zero coverage D atom sticking probabilities between 0.25 and 0.5, where the variation is from graphite sample-to-sample.[24] For H, the sticking probabilities are about 0.4, with similar sample-to-sample variation. The atomic beams used in the experiments are reported to have Maxwellian energy distributions which peak around 0.2 eV.[24] If we average our 3D+Q results at 1 ps over a Maxwell−Boltzmann distribution at 2000 K, we estimate that the sticking probabilities for H and D are 0.024 and 0.050, respectively. While these estimates are well below the experimental values, they represent a lower bound. As discussed earlier, increasing the number of lattice modes should significantly increase the amount of trapping at longer times. In addition, our arbitrary choice of 1 ps to estimate the sticking may be too large, our barrier might be too high, and/or our incident energy distribution might be too low in energy. If so, correcting these would also increase the sticking probability. Finally, in a recent DFT study, Allouche and coworkers have suggested that, following the adsorption of an H atom onto the graphite plane, it becomes energetically favorable for three additional H atoms to chemisorb about this H.[13] It is possible that the cross sections for the adsorption of these three additional H atoms are larger than for the initial H and that the H sticking probability at true zero H coverage is much smaller than the reported value based on larger coverages.

Given the experimental interest in this problem, we are implementing more detailed studies. First, an accurate force field for the motion of the graphite lattice is now being incorporated into our current scattering model. This will allow us to more accurately describe the relaxation of the C−H stretch. It will also allow us to realistically examine temperature effects by including low frequency lattice modes. Models that include only a small number of lattice atoms, as in this study, contain only higher frequency vibration modes that are not populated at typical experimental temperatures. While limited in dimensionality, further quantum studies would be helpful. Quantum effects are important for this problem, and the agreement between the classical and quantum approaches, for the lower dimensional collinear model, was far from perfect. Computing the trapping resonances for the 3D system would help us to better understand the trapped state, as well as the structure in Figures 7 and 8. Given the cylindrical symmetry of our 3D PES with respect to the bonding carbon, we should be able to quantum mechanically compute cross sections for H-graphite trapping on a static lattice using methods developed for the study of Eley−Rideal reactions.[35,36] It should be possible to extend this to include one or two lattice modes.

Acknowledgment. B.J. gratefully acknowledges support from the Division of Chemical Sciences, Office of Basic Energy Sciences, Office of Energy Research, U. S. Department of Energy, under Grant No. DE-FG02-87ER13744.

Appendix A

In this Appendix, we provide the remaining details necessary to fully define the PES described in the main text. The collinear term, $V_0(z_H, z_C)$, was found to be well-described by the following form:

$$V_0(z_H,z_C) = (C_1(z_C) + D_0(z_C))[\exp[-2A(z_H - Z_M(z_C))] - 2\exp[-A(z_H - Z_M(z_C))]] + C_1(z_C) + C_2(z_C) \times \exp[-B(z_C)(z_H - Z_G(z_C))^2] \quad \text{(A1)}$$

TABLE 1: Parameters Defining the Potential Energy Surface Described in the Text and Appendix A

$a_f = 1.40$ Å^{-1}	$b_f = 1.65$ Å^{-1}	$c_f = 2.90$ Å^{-1}	$\rho_f = 1.00$ Å
$D_i = 0.00775$ eV	$\alpha_i = 0.954$ Å^{-1}	$a_i = 4.01$ Å	$k_C = 14.262$ eV/Å^2
$b_s = 6.00$ Å^{-1}	$\rho_s = 0.53$ Å	A = 2.276 Å	

The z_C-dependent terms in eq A1 have the following forms and were fit to the computed DFT energies:

$$C_1 = k_C z_C^2/2 - 0.00326 \quad \text{(A2)}$$

$$D_0 = 0.475 + 0.988z_C - 1.392z_C^2 + 0.028z_C^3 - 1.888z_C^4 + 0.11\exp[-8.0(z_C - 0.280)^2] \quad \text{(A3)}$$

$$Z_M = 0.874z_C + 1.174 \quad \text{(A4)}$$

$$C_2 = 0.309\exp[-2.742(z_C - 0.262)] + 0.031 \times \exp[3.184(z_C - 0.187)] + 0.020\exp[-20.0(z_C - 0.100)^2] \quad \text{(A5)}$$

$$B = 4.002\exp[1.260(z_C - 0.587)] \quad \text{(A6)}$$

and

$$Z_G = 1.992z_C + 1.461 \quad \text{(A7)}$$

where z_C is in Å, C_1, C_2, and D_0 are in eV, Z_M and Z_G are in Å, B is in Å^{-2}, and A and k_C are defined in Table 1.

The radial force constant was computed via DFT at several values of z_H and z_C. The following two-Gaussian form for $k_\rho(z_H, z_C)$ was then fit to these values:

$$k_\rho(z_H, z_C) = 3.866\exp[-17.039(z_C - 0.538)^2 + 0.313(z_C - 0.538)(z_H - 2.004) - 4.480(z_H - 2.004)^2] + 4.31741\exp[-11.932(z_C - 0.287)^2 + 18.541(z_C - 0.287)(z_H - 1.541) - 14.537(z_H - 1.541)^2] \quad \text{(A8)}$$

where z_C is in Å and k_ρ is in eV/Å^2. The remaining parameters are listed in Table 1.

References and Notes

(1) Küppers, J. *Surf. Sci. Rep.* **1995**, *22*, 249.
(2) Meregalli, V.; Parrinello, M. *Appl. Phys. A* **2001**, *72*, 143.
(3) Hollenbach, D. H.; Salpeter, E. E. *J. Chem. Phys.* **1970**, *53*, 79; *Astrophys. J.* **1971**, *163*, 155.
(4) Fitzpatric, E. L.; Masa, D. *Astrophys. J. Suppl.* **1990**, *Series 72*, 163. Papoular, R.; Conrad, J.; Guillois, O.; Nenner, I.; Reynaud, C.; Rouzaud, J.-N. *Astron. Astrophys.* **1996**, *315*, 222.
(5) Jeloaica, L.; Sidis, V. *Chem. Phys. Lett.* **1999**, *300*, 157.
(6) Sidis, V.; Jeloaica, L.; Borisov, A. G.; Deutscher, S. A. *Molecular Hydrogen in Space*; Cambridge Contemporary Astrophysics Series;Combes, F., Pineau des Forêts, G., Eds.; Cambridge University Press: Cambridge, 2000; pp 89−97.
(7) Sha, X.; Jackson, B. *Surf. Sci.* **2002**, *496*, 318.
(8) Ferro, Y.; Marinelli. F.; Allouche, A. *J. Chem. Phys.* **2002**, *116*, 8124.
(9) Yang, F. H.; Yang, R. T. *Carbon* **2002**, *40*, 437.
(10) Miura, Y.; Kasai, H.; Diño, W. A.; Nakanishi, H.; Sugimoto, T. *J. Phys. Soc. Jpn.* **2003**, *72*, 995.
(11) Ferro, Y.; Marinelli. F.; Allouche, A. *Chem. Phys. Lett.* **2003**, *368*, 609.
(12) Ferro, Y.; Marinelli. F.; Allouche, A.; Brosset, C. *J. Chem. Phys.* **2003**, *118*, 5650. Ferro, Y.; Marinelli. F.; Jelea, A.; Allouche, A. *J. Chem. Phys.* **2004**, *120*, 11882.
(13) Allouche, A.; Ferro, Y.; Angot, T.; Thomas, C.; Layet, J.-M. *J. Chem. Phys.* **2005**, *123*, 124701.
(14) Parneix, P.; Bréchignac, Ph. *Astron. Astrophys.* **1998**, *334*, 363.
(15) Kim, Y. K.; Ree, J.; Shin, H. K. *Chem. Phys. Lett.* **1999**, *314*, 1.

(16) Farebrother, A. J.; Meijer, A. J. H. M.; Clary, D. C.; Fisher, A. J. *Chem. Phys. Lett.* **2000**, *319*, 303.
(17) Jackson, B.; Lemoine, D. *J. Chem. Phys.* **2001**, *114*, 474.
(18) Rutigliano, M.; Cacciatore, M.; Billing, G. D. *Chem. Phys. Lett.* **2001**, *340*, 13.
(19) Meijer, A. J. H. M.; Farebrother, A. J.; Clary, D. C.; Fisher, A. J. *J. Phys. Chem. A* **2001**, *105*, 2173.
(20) Sha, X.; Jackson, B.; Lemoine, D. *J. Chem. Phys.* **2002**, *116*, 7158.
(21) Morisset, S.; Aguillon, F.; Sizun, M.; Sidis, V. *Phys. Chem. Chem. Phys.* **2003**, *5*, 506; *Chem. Phys. Lett.* **2003**, *378*, 615; *J. Phys. Chem. A* **2004**, *108*, 8571.
(22) Martinazzo, R.; Tantardini, G. F. *J. Phys. Chem. A* **2005**, *109*, 9379.
(23) Morisset, S.; Aguillon, F.; Sizun, M.; Sidis, V. *J. Chem. Phys.* **2004**, *121*, 6493; **2005**, *122*, 194702.
(24) Zecho, Th.; Güttler, A.; Sha, X.; Jackson, B.; Küppers, J. *J. Chem. Phys.* **2002**, *117*, 8486.
(25) Zecho, Th.; Güttler, A.; Sha, X.; Lemoine, D.; Jackson, B.; Küppers, J. *Chem. Phys. Lett.* **2002**, *366*, 188.
(26) Zecho, Th.; Güttler, A.; Küppers, J. unpublished material.
(27) Perry, J. S. A.; Price, S. D. *Astrophys. Space Sci.* **2003**, *285*, 769.
(28) Sha, X.; Jackson, B.; Lemoine, D.; Lepetit, B. *J. Chem. Phys.* **2005**, *122*, 014709.
(29) Kresse, G.; Furthmuller, J. *Phys. Rev. B* **1996,** *54*, 11169.
(30) Kresse, G.; Furthmuller, J. *Comput. Mater. Sci.* **1996**, *6*, 15.
(31) Kresse, G.; Hafner, J. *Phys. Rev. B* **1993**, *47*, 558; **1994**, *49*, 14251.
(32) Perdew, J. P. In *Electronic Structure of Solids*; Ziesche, P., Eschrig, H., Eds.; Akademie-Verlag: Berlin, 1991; p11.
(33) Siebentritt, S.; Pues, R.; Rieder, K.-H.; Shikin, A. M. *Phys. Rev. B* **1997**, *55*, 7927.
(34) Ghio, E.; Mattera, L.; Salvo, C.; Tommasini, F.; Valbusa, U. *J. Chem. Phys.* **1980**, *73*, 556.
(35) Persson, M.; Jackson, B. *J. Chem. Phys.* **1995**, *102*, 1078.
(36) Lemoine, D.; Jackson, B. *Comput. Phys. Commun.* **2001**, *137*, 415.